Self-Assembly Behavior of Oppositely Charged Inverse Bipatchy Microcolloids

Fatemeh Naderi Mehr, Dmitry Grigoriev, Rebecca Heaton, Joshua Baptiste, Anthony J. Stace, Nikolay Puretskiy, Elena Besley,* and Alexander Böker*

A directed attractive interaction between predefined "patchy" sites on the surfaces of anisotropic microcolloids can provide them with the ability to self-assemble in a controlled manner to build target structures of increased complexity. An important step toward the controlled formation of a desired superstructure is to identify reversible electrostatic interactions between patches which allow them to align with one another. The formation of bipatchy particles with two oppositely charged patches fabricated using sandwich microcontact printing is reported. These particles spontaneously self-aggregate in solution, where a diversity of short and long chains of bipatchy particles with different shapes, such as branched, bent, and linear, are formed. Calculations show that chain formation is driven by a combination of attractive electrostatic interactions between oppositely charged patches and the charge-induced polarization of interacting particles.

1. Introduction

Patchy particles, as particular types of anisotropic microcolloids, are increasingly attracting attention due to their nonuniform, often asymmetric shape, and characteristic properties. They are designed for controlled self-assembly allowing a diversity of complicated target superstructures, such as chains and rings, as well as 2D and 3D structures, such as squares, pyramids, tetrahedra, twisted shapes, and even diamonds.[1–3] Since not all of these structures

Dr. F. Naderi Mehr, Dr. D. Grigoriev, Dr. N. Puretskiy, Prof. A. Böker
Fraunhofer Institute for Applied Polymer Research IAP
Geiselbergstr. 69, Potsdam 14476, Germany
E-mail: alexander.boeker@iap.fraunhofer.de
R. Heaton, J. Baptiste, Prof. A. J. Stace, Prof. E. Besley
School of Chemistry
University of Nottingham
University Park
Nottingham NG7 2RD, UK
E-mail: Elena.Besley@nottingham.ac.uk
Prof. A. Böker
Chair of Polymer Materials and Polymer Technologies
University of Potsdam
Institute of Chemistry
Karl-Liebknecht-Str. 24–25, Potsdam 14476, Germany

have been achieved experimentally, considerable interest is focused on the mechanism of their formation and on the corresponding interactions between patchy particles. Size, number, and spatial distribution of patches play a crucial role in the formation of the final constructs; this stimulates computational simulations aimed at predicting the form and 3D of the resulting structures by changing the patch parameters.[4–6] Simulations by Guo and co-workers[7,8] have shown that DNA strand-like helices could be generated through the assembly of tripatchy particles and the distribution of patches defines the diameter of the final helix. Furthermore, a simpler model has been developed for the formation of polymer-like chains of bipatchy particles with patches at the particle poles.[9]

In addition to these computational simulations, patchy particles with two (Janus particles) or more patches have also been prepared in recent experimental work.[10,11] However, self-assembly of these particles into chains or helices has not been reported.[10,12] Patchy colloids with more than two patches can be produced by the colloidal fusion of a liquid core out of a pressure-deformed cluster of particles.[10] The chemistry of the patches on the particles can be used to control the strength and the directionality of the interactions between colloidal building blocks[13] when symmetrical clusters made from just a few spherical colloidal particles (called as "colloidal molecules," CMs) are created.

A disadvantage of the method mentioned above[10] is its limited applicability and the lack of chemical and physical diversity of the patches. A further method, microcontact printing (μCP) or sandwich microcontact printing, has been developed for the preparation of more than one patch in a simple one-step process. This approach was recently established for the attachment of an amino-functionalized ink onto polymer particles synthesized via an epoxy ring-opening reaction,[14–17] or preparation of trifunctional Janus beads via thiol-ene chemistry that were able to selectively bind various proteins from their mixture on specifically modified orthogonal patches.[18] It has also been shown that polymeric ink with a high molecular weight, e.g., branched polyethylenimine (PEI), can be electrostatically attached to the surface of silica particles. A variety of patches from 2D and 3D to those with striped patterns have been formed via microcontact printing with wrinkled polydimethylsiloxane (PDMS) stamps. Despite their shape diversity, all of these patches were uniform in other properties and identically charged.[19–21] Chemical or physical interactions between patches, e.g., covalent bound, van der Waals, and electrostatic

interactions define the reversibility of the formation of any desired structure. In contrast to covalent bonds, electrostatic interactions have an advantage in that they serve as reversible links for the connection of patchy particles. In this work, we have used sandwich microcontact printing to produce bipatchy melamine formaldehyde (MF) microparticles with oppositely charged patches consisting of either poly(methyl vinyl ether-alt-maleic acid) (PMVEMA) or PEI. The successful attachment of these polymers to the particle poles is demonstrated by different microscopic methods, where the measurements show that we have improved the yield of bipatchy particles. Thereafter, we concentrate on the study of the self-aggregation behavior of the patchy particles in solution. From a comprehensive statistical analysis of variable chains, such as short and long, branched, bent and linear, we can show that chain formation through the connections between patches is due to electrostatic attractions between oppositely charged patchy particles. These interactions can be weakened or even eliminated by increasing the ionic strength of the medium.

2. Bipatchy Particles with Two Oppositely Charged Patches

Multivalent, oppositely charged polymers, PMVEMA as well as PEI can be attached to the surfaces of MF particles as the isoelectric point (IEP) of the latter has been found to have approximately neutral pH.[22] A localized change in the pH to either acidic or basic at the contact surface of the MF particles and the polymeric inks leads to their attachment through electrostatic attraction (**Figure 1**a).

For sandwich µCP, two stamps were spin coated with water solutions of PMVEMA and PEI, respectively. A monolayer of particles, prepared by drop casting a dispersion of MF particles on a glass substrate, was pressed against the first stamp, which was spin coated with PMVEMA. To generate second patches made of PEI on the opposite side of MF particles, the second stamp was pressed against the first stamp with particles immersed in PMVEMA layer. Finally, bipatchy particles were released in acetone from the second stamp.
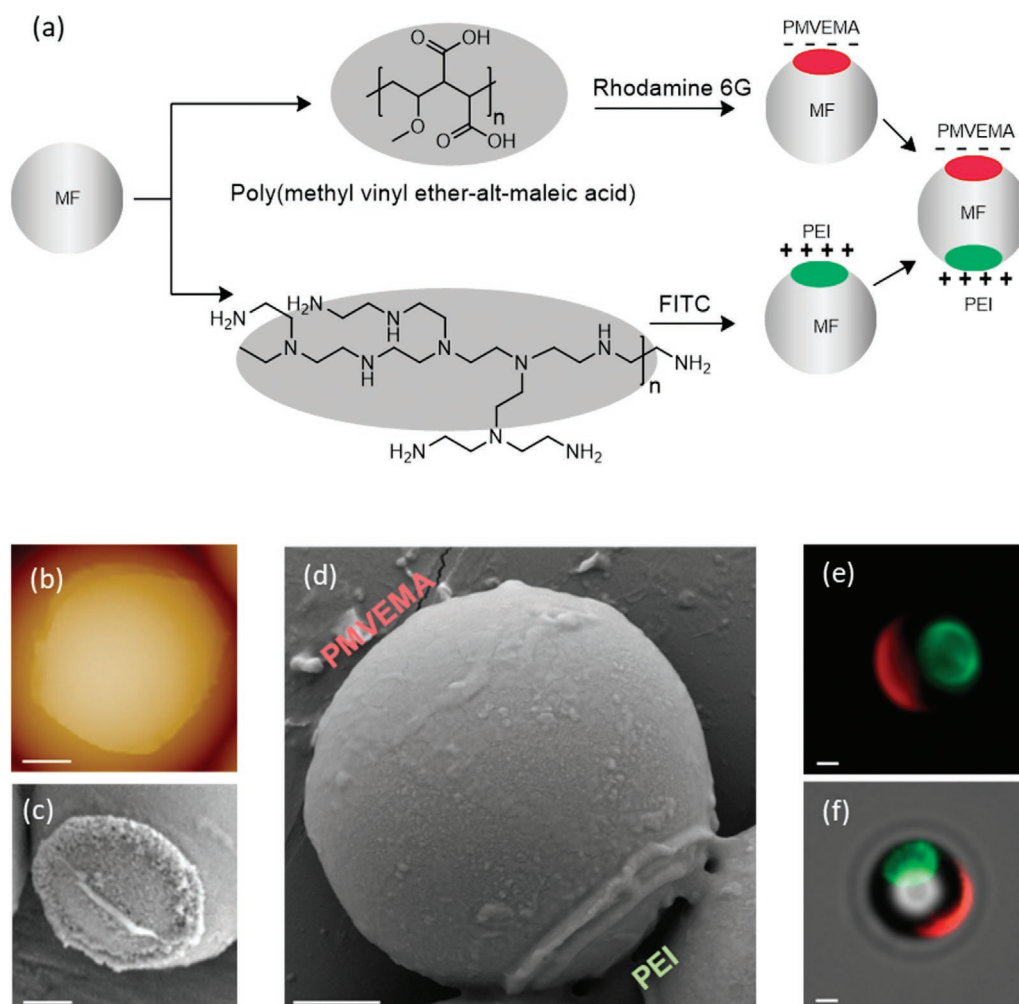

Figure 1. a) Scheme of the generation of oppositely charged patches on the surface of an MF particle made of prelabeled PMVEMA and PEI with Rhodamine 6G and FITC, respectively. b) SFM height image of a PMVEMA patch. c) SEM image of a PEI patch. d) SEM image and e,f) fluorescence and the overlaid microscope images of bipatchy MF particles with patches made of PMVEMA and PEI that are coloured red and green, respectively. Scale bars:1 µm.

**ADVANCED
SCIENCE NEWS**

www.advancedsciencenews.com

NANO · MICRO
small

www.small-journal.com

2.1. Characteristics and the Yield of Patchy Particles

The patchy particles were characterized by various microscopy methods (Figure 1b–f). To achieve a clear visualization of the patches for fluorescence microscopy, the polymers PMVEMA and PEI were labeled with Rhodamine 6G and fluorescein isothiocyanate (FITC) tags, respectively. Information about the morphology and surface properties of the patches was obtained by scanning electron microscopy (SEM) and scanning force microscopy (SFM). As one can clearly see (Figure 1b–d), there are distinct borders between the patches and the bare surface of particles, enabling an exact measurement of the patch size. Using several tens of SEM and SFM images, the following values for patch size were obtained: 2.33 ± 0.16 and 2.4 ± 0.2 µm for PEI and PMVEMA patches, respectively.

To determine the yield of the bipatchy particles by sandwich µCP, a sample of the patchy particles was observed by fluorescence microscopy and the individual particles counted manually. The yield was then calculated from the number of bipatchy particles divided by the total number of non-, mono-, and bipatchy particles. To check, if the calculated yield of this arbitrarily chosen small sample was representative of the entire batch, a hemocytometer counting chamber was used, where the total number of particles in each batch (n_{batch}) could be determined. Since the initial number of untreated MF particles (N), which were drop casted on the glass substrate as a monolayer used for sandwich µCP, is known, the accuracy of the statistics can also be defined. According to the literature, the sample size of a population is related to the reliability of the statistics. For a desired precision (e) the sample size can be calculated for a known population number as follows[23]

$$n_{batch} = \frac{N}{1 + N(e)^2} \tag{1}$$

For instance, to have a simple and fast comparison of the obtained yield with and without using the Hemocytometer, two independent samples of PMVEMA monopatchy particles were prepared. Our investigations showed that the calculated yield using the counting chamber was 91%, which was in good agreement with the 90% yield found by counting a smaller sample. In the counting chamber, 1 µL of the dispersion of particles was deposited and counted; this was then multiplied by the total volume of 50 µL, to calculate the value of n_{batch}. The value of N can then be calculated by dividing the total mass of the drop-casted MF particles by the mass of a single MF particle. By drop casting 5 µL of a 1 wt% dispersion of particles, the total mass of MF particles was 5×10^{-5} g. Using a diameter of 5.17 µm and a density of 1.51 g cm^{-3}, the mass of an individual particle was calculated to be 109.83×10^{-12} g. Replacing the known values of $n_{batch} = 15\,334$ and $N = 455\,249$ in Equation (1), the precision was calculated as 99% (± 0.008).

To study the effects of concentration of the polymer solutions used for µCP on the yield of bipatchy particles, PMVEMA and PEI were used with equal concentrations at the level of 1, 2, and 3 wt%. An increase from 1 to 2 wt%

Table 1. Yield of bipatchy particles as a function of the concentration of a polymer solution which was spin-coated on the stamp for µCP.

Concentration of PMVEMA and PEI [wt%]	Number of bipatchy particles	Total number of particles	Yield [%]
1	162	220	74
2	170	207	82
3	30	145	21

resulted in an increase in the number of patchy particles, whereas a further increase to 3 wt% led to a decrease in yield (**Table 1**). The yield of bipatchy particles is the product of two individual yields of monopatchy particles with patches of PMVEMA and subsequently PEI during the printing process. For example, a reduction in the yield of bipatchy particles to 21% at 3 wt% concentration is the consequence of the small yield (24%) of PMVEMA patches, despite the relatively high yield (85%) of PEI patches at this concentration. The reason of the reduced yield of PMVEMA monopatchy particles is that the pH of higher concentrations of PMVEMA tends toward more acidic values, which are very close to the IEP of the PDMS stamp (pH $\approx$ 2).[22,24] Therefore the adhesion of PMVEMA to PDMS was stronger and the yield of corresponding patches on MF particles decreased. Finally, as standards for further investigations, the polymer inks at 2 wt% were used due to the satisfactory yield of bipatchy particles at this concentration.

2.2. Electrostatic Interactions between Patchy Particles

2.2.1. Experimental Results on the Bipatchy Particles Self-Aggregation

Self-aggregation behavior in solutions of bipatchy particles was followed by fluorescence microscopy. To avoid the influence charge on the surfaces of MF particles might have on the interactions between patches, the pH value of the solution was maintained close to the IEP of MF particles. To this end, a mixture of ethanol-water (90:10) was used as a dispersant, where the pH$_e$ 8.9 corresponds to the IEP of the MF particles.[22] Since the difference in refractive index between this medium and the refractive index of the MF particles is smaller than in the case of pure water, the clarity of fluorescence microscope images of the bipatchy particles was improved. Only structures in an equilibrium state and settled on the bottom of the microscopy cuvette were counted and recognized in the statistical processing.

Since the yield of bipatchy particles by sandwich µCP is lower than 100%, self-aggregation occurs in a mixture of mono- and bipatchy particles. According to the rules of probability, six connection types of the patchy particles can be formed through accidental collisions between of patchy and nonpatchy surfaces. The predicted occurrence of each connection type will then be one-sixth ($\approx$17%). Comparison with the statistical values of the observed patchy particles via sandwich µCP shows a very large difference in the fraction of connection type (PMVEMA-PEI), which is formed due to the oppositely charged patchy surfaces

**ADVANCED
SCIENCE NEWS**
www.advancedsciencenews.com
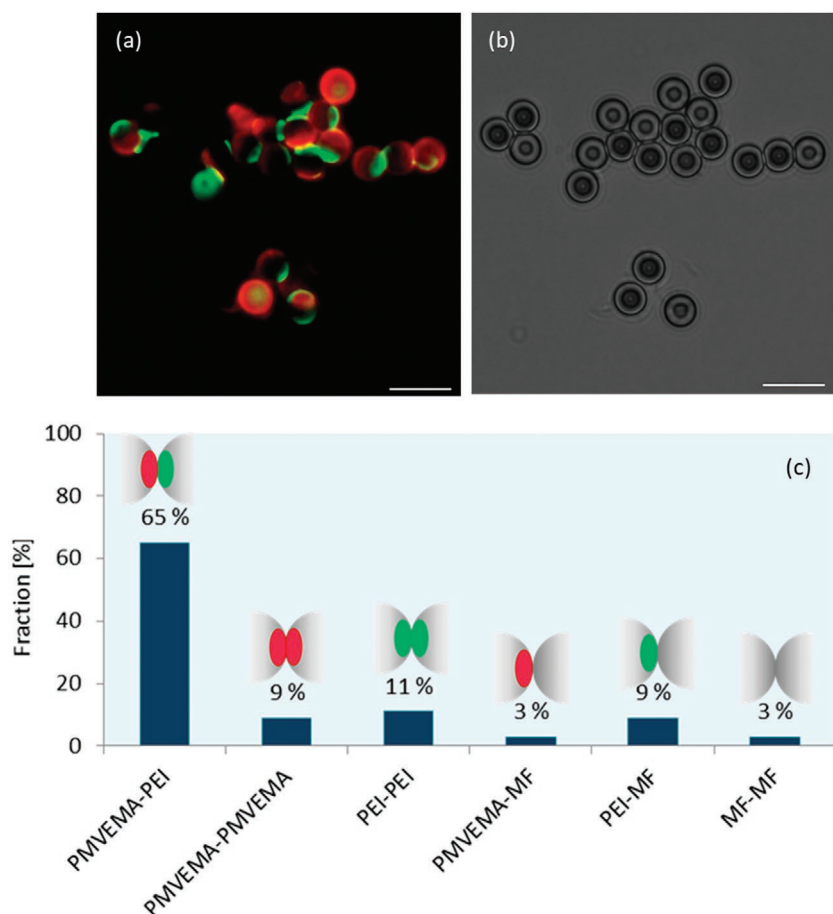
NANO · MICRO
small
www.small-journal.com

Figure 2. a) Fluorescence and b) optical microscope images of the self-assembly of bipatchy particles. c) Six possible connection types which could be formed via random interactions between patchy and nonpatchy surfaces of particles, together with statistics of experimentally observed connections in the aggregates formed by MF bipatchy particles. The fraction of PEI patch interactions is larger than the fraction of PMVEMA interactions due to the higher yield of PEI patches.[20]

2.2.2. Change of the Ionic Strength

The self-aggregation of bipatchy particles via electrostatic interactions can be extinguished by a change in the ionic strength. With an addition of a saturated solution of NaCl to the patchy particles, electrostatic interactions between oppositely charged PEI and PMVEMA patches can be reduced through dissociation of the salt, such that long chains break down to form short chains and single particles. This effect could be seen by optical as well as fluorescence microscopy or even with the unaided eye (**Figure 4**a–d).

As a reference, the statistics of the short and long chains, as well as the single particles of untreated MF particles, were compared to the statistics of the bipatchy particles before and after the addition of NaCl solution. As expected, the number of single particles has increased; however, the new value is essentially lower than the number of singlets in the reference sample (Figure 4e). The residual small fraction of aggregated particles might reveal the presence of other attractive interactions such as hydrogen bonds or Van der Waals forces; however, weak electrostatic interactions may still exist between charged patch surfaces of the bipatchy particles. More details of the statistics are available in Table S2 in the Supporting Information.

2.2.3. Theoretical Considerations of Patchy Particles Self-Aggregation in Comparison with Experimental Results

Self-aggregation of patchy particles can be better understood through *the accurate evaluation* of the electrostatic interaction energy between pairs of charged patchy particles in different relative orientations. In the general case of a two-body electrostatic interaction between polarizable (dielectric) particles, electric charge on one of the particles creates an electric field that induces a redistribution of surface charge and the polarization of bound charge on a second particle, which, in turn, generates its own electric field, prompting complementary polarization effects on the first particle. This iterative process results in an equilibrium state where both particles acquire a static charged configuration that can lead to either an attractive or repulsive force between the interacting particles, which can be readily calculated analytically.[25]

In the considered case of particles having patches of different charge and dielectric constant, a general solution[26] based on an integral equation approach to calculating electrostatic interactions between many dielectric spherical particles has been used. The solution treats any number of interacting particles of arbitrary size, charge, position, and dielectric constant, embedded in a homogeneous dielectric medium. In our work, each bipatchy particle is represented by three
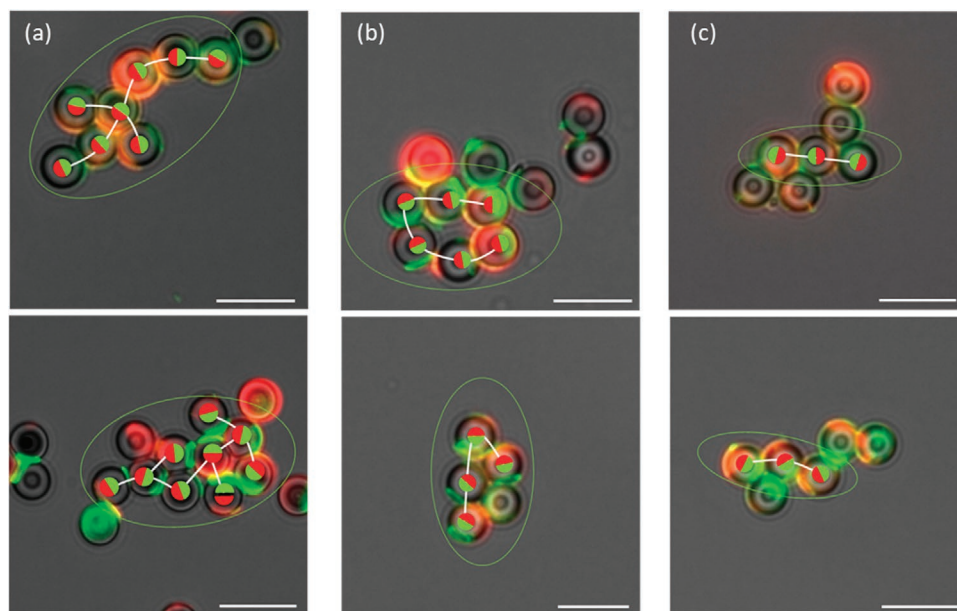
(**Figure 2**). The statistics of the connection types is summarized in the supporting data (Table S1, Supporting Information). As a result, a variety of short and long chains were spontaneously formed via connection type (PMVEMA-PEI) between two, three, or more patchy particles, respectively. From the morphological viewpoint, their steric structures differ from chain to chain and so branched, bent, and linear forms could be observed by fluorescence microscopy (**Figure 3**). To improve the visualization, fluorescence and optical microscope images of the chains are overlaid and connections between the bipatchy particles represented by white lines, and oppositely charged PMVEMA and PEI patches are highlighted with red and green half-circles, respectively. The statistics of the chains formed via PMVEMA-PEI connections in terms of their lengths and shapes are summarized (**Table 2**). Assuming bent chains are a simple kind of branched chain, the statistics show a higher fraction of long and branched chains. Thus, in the absence of external physical forces, e.g., mechanical, the only driving force for the self-aggregation of the patchy particles into chains via PMVEMA-PEI connections is an attractive electrostatic interaction between oppositely charged patch surfaces.

Figure 3. Overlay of fluorescence and optical microscope images of a) the branched, b) bent, and c) linear chains, which are formed via electrostatic attraction between oppositely charged PMVEMA and PEI patches. For a better visualization, connections between bipatchy particles are represented with white lines, PMVEMA and PEI patches are additionally highlighted with red and green colored half-circles, respectively. Scale bars: 10 μm.

spheres: the central sphere corresponding to the MF carrier and two smaller ones on either side representing the patches. The input parameters, summarized in **Table 3**, were either measured experimentally (sizes of patches and particles) or derived on the basis of well-established theoretical concepts using the data from the literature (e.g., charges on patches were calculated from the data on electrophoretic mobility or zeta-potential according to the Smoluchowski approximation, see ref. [22] and references therein). These parameters were used in computation of the surface charge distribution on the particles and the electrostatic interaction forces driving their self-aggregation at all relative orientations and separations. The action of charges under their mutual polarization influence is obtained from Gauss's law that couples uniquely the surface potential with the distribution and magnitude of electrical charge on the surface of the particles. The effect of the surface charge is integrated to numerically obtain the electrostatic force acting on the particles at arbitrary separations and orientations using a Galerkin approximation of an integral equation formulation.[26] The effect of the solvent on the self-assembly behavior is captured by the dielectric constant of the ethanol: water (90:10) medium, taken to be 30.05, as no charge screening is present in the solution (large Debye screening length). The effect of an increased ionic strength on self-aggregation behavior of patchy particles has been studied previously in ref. [22] by adding a saturated solution of NaCl in ethanol/water (90:10).

The strongest attractive interaction energy, below −0.05 fJ at short separation distances, is predicted for a pair of bipatchy particles with the PMVEMA-PEI connection type (**Figure 5**a); this interaction is dominated by a Coulomb attractive force between patches of opposite charge, which constitutes 65% of the overall interaction outcomes found experimentally (see Figure 2c). Similar electrostatic behavior is observed if a monopatchy and a bipatchy particle interact directly through either PMVEMA-PMVEMA, PEI-PEI, or PMVEMA-PEI connections (Figure S1, Supporting Information). Much weaker attractive interactions (Figure 5b), attenuated by polarization of neutral MF particles by the charged patches and polarization effects of the solvent,[27] account for a further 12% of the attractive interaction outcomes observed in the experiment (Figure 2c). Note that this attractive regime only occurs if the patches on the opposite (outer) sides of the interacting pair are identical. The overall interaction between a bipatchy particle and a monopatchy particle remains repulsive if the outer patches have different sign of charge and chemical composition, which affects the value of the dielectric constant and hence the strength of the total electrostatic force and charge induced polarization.

Although electrostatic interactions between two individual bipatchy particles with PMVEMA-PMVEMA and PEI-PEI patch contacts are always repulsive, these connections might be still observed experimentally in small self-assembled clusters, such as those shown in Figure 3. Such connections could arise from the complexity of subtle changes in the density of charge residing on the surface of each particle as a consequence of charge-induced polarization effects, as seen in many-body systems.[28,29] An attraction between objects carrying the same sign of charge is even possible in the pairwise interaction and
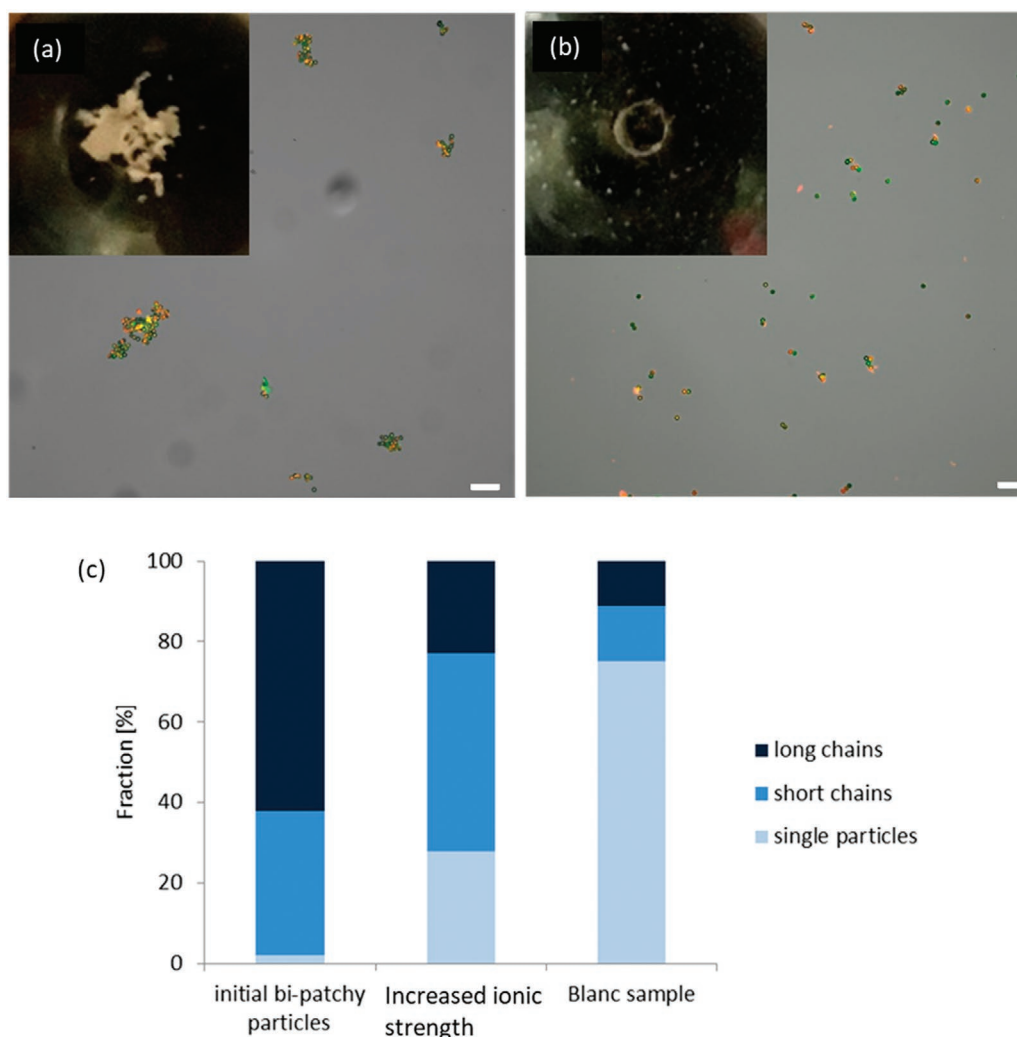
Table 2. Statistics for short (two to three particles) and long (more than three particles) chains as well as branched, bent, and linear chains.

Chains	Short	Long	Total	Branched	Bent	Linear	Total
Number (fraction)	102 (34%)	196 (66%)	298 (100%)	129 (42%)	120 (39%)	58 (19%)	307 (100%)

ADVANCED
SCIENCE NEWS
www.advancedsciencenews.com

NANO · MICRO
small
www.small-journal.com

Figure 4. Overlay of the optical and fluorescence microscope images of the bipatchy particles a) before and b) after addition of a solution of NaCl. The elimination of self-aggregation can also be observed by the unaided eye. In solution, the white sediment of the large aggregates at the bottom of the Eppendorf tube (inset (a)) converts upon increase of the ionic strenght to a turbid dispersion of small aggregates and single particles (inset (b)). c) Statistics for long and short chains as well as single particles in a dispersion of bipatchy particles before and after addition of the NaCl solution in comparison with the statistics obtained for a sample of untreated MF particles. Scale bars: 25 µm.

results from a mutual polarization of charge density close to the region where they are in contact.[28] To generate an attractive interaction between like-charged objects it is not only necessary for one object with a high charge density to polarize another, but there has to be a reciprocal displacement of density on the second object, too.[28] In the case of small clusters (many-body systems) as observed here, the polarization of charge density and its mutual redistribution is essentially more complex, leading finally to the induction of an opposite charge on the location close to or within one of the apparently equally charged patches.
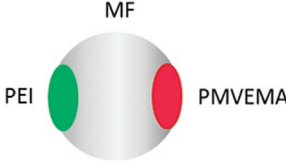
The rotational barrier between the repulsive PMVEMA-PMVEMA and PEI-PEI orientations and the stable the PMVEMA-PEI orientation decreases with distance between the interacting particles, but remains higher than 0.04 fJ even when the surface-to-surface separation distance reaches 4 µm (Figure S2, Supporting Information). Such a high

barrier eliminates the possibility of a thermally induced rotation of particles in the ethanol-water medium during self-assembly.

3. Conclusion and Outlook

We have successfully fabricated oppositely charged polymeric patches on the surfaces of polymer MF particles with a reasonable yield. The effect of the concentration of the polyelectrolyte ink on the yield of the bipatchy particles has been studied, and a standard concentration of 2 wt% has been chosen for further investigation. In solution, the bipatchy particles spontaneously self-aggregated and mostly connect via PMVEMA and PEI interactions. As a result, a variety of short and long chains of bipatchy particles grew, which could be branched, bent, or linear. In addition to electrostatically driven attraction between

ADVANCED
SCIENCE NEWS
www.advancedsciencenews.com

NANO · MICRO
small
www.small-journal.com

Table 3. The parameters used in the computations of electrostatic interaction energies: k is the dielectric constant, a is the radius, and q is the charge; k_{medium} is 30.05 (90:10 mixture of ethanol and water). A particle graphic representation is also included for clarity.

MF

PEI   PMVEMA

Substance	k	a [μm]	q [fC]
MF	8.0	2.59	0
PEI	3.8	1.295	+0.734
PMVEMA	3.5	1.295	−0.923

patches of opposite charge, attractive forces also arise through charge-induced polarization interactions between charged patches and the neutral surfaces of particles; the latter amounts to 12% of the interaction outcomes, for connection types PMVEMA-MF and PEI-MF. These attractive forces are driven by an instantaneous redistribution of charge on the neutral surfaces of interacting particles due to the presence of a charged patch in close proximity; however, these forces are significantly weaker (up to an order of magnitude) than those due to opposite charge attraction. Moreover, 20% of the observed interactions are connections between initially equally charged patches PMVEMA-PMVEMA and PEI-PEI and are a consequence of charge-induced polarization and charge redistribution effects in many-body systems.

To understand further the relation between electrostatic interactions and the formation of chains, a variety of statistics have been performed, with the reliability of the latter being tested against a known sample size. To examine if the formation of chains via oppositely charged patches is as a result of electrostatic interactions, the ionic strength of the dispersion has been changed through the addition of a saturated solution of NaCl. As a result, self-aggregation was either eliminated or weakened due to reduced electrostatic attraction. However, a

comparison of statistics for the latter with a reference sample of MF particles shows a higher number of short chains even after the addition of the salt. This observation may indicate that there are still other types of interaction between bipatchy particles, for example, hydrogen bonds, which were not influenced by a change in ionic strength.

Almost half of all connections observed in aggregates are connections where directional contacts between oppositely charged patches are absent. This is the most important feature of electrostatic interaction as the main driving force for the self-assembly of patchy particles: polarization and redistribution of charge especially in many-body systems leads to a much more complicated localization of charge in these systems (not only on the patches) and to a "blurring" of directional interactions. This effect is further enhanced by the relatively large size of patches especially in comparison with the size of patchy particles, causing a more complex spatial distribution of the electric field when compared to point charges. Also, the lower charge density in patches compared to point charges leads to a less expressed polarization of induced charges and to stronger delocalization.

A theoretical calculation of electrostatic interactions between patchy microparticles used experimentally demonstrated a significant prevalence of electrostatic energy over the energy of thermal motion (kT); however, the barrier is of the same order of magnitude as the kinetic energy of particle movement in, for example, a local laminar flow.

These observations show that by-patchy microparticles with oppositely charged patches, obtained by microcontact printing, are less suitable for directed self-assembly than particles with other types of patch-to-patch binding (covalent, hydrophobic, etc.). This conclusion is a consequence of the complicated electrostatic interactions and redistribution of initial charge and charge induced polarization found in complex many-body systems. To improve the directional character of particle self-assembly via electrostatics, the size of particles should be decreased to submicrometer to essentially reduce disruption from their kinetic energy due to randomly distributed mechanical noise. In addition, the size of charged patches produced by microcontact printing is too large compared to the particles themselves. The charged patches should be more localized and
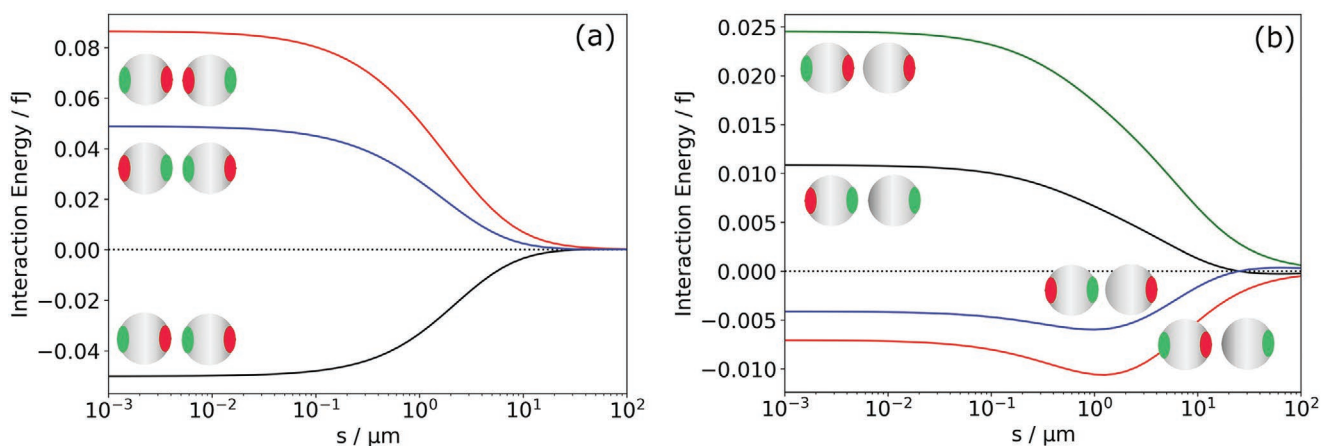

Figure 5. Electrostatic interaction energy (in fJ) as a function of the surface-to-surface separation between: a) two bipatchy particles and b) bipatchy and monopatchy particles. PMVEMA and PEI patches are highlighted by red and green colors, respectively.

possess higher charge densities in order to improve the directionality of electrostatically driven interactions.

4. Experimental Section

Materials: Poly(methyl vinyl ether alt maleic acid) (PMVEMA) with M_w of 1980 kDa and branched poly(ethyleneimine) (PEI) with M_w of 600–1000 kDa, fluorescein isothiocyanate, rhodamine 6G, and sodium chloride were supplied by Sigma-Aldrich. Acetone and ethanol of p.a. quality were purchased from VWR International GmbH. MF particles with an average size of 5.17 ± 0.09 µm were synthesized by Microparticles GmbH. The polydimethylsiloxane PDMS kit, Sylgard 184—silicone elastomer, containing the monomer and curing agent was obtained from Dow Corning.

Preparation of the Inked PDMS Stamps and Monolayer of Particles: To synthesize PDMS, a 10:1 mixture of monomer and crosslinker was poured into a rectangular Petri dish to form a polymer matrix with a thickness of ≈3 mm. After letting the mixture rest overnight to remove air bubbles, it was heated to 80 °C for 2 h. The crosslinked PDMS was then cut into 1 cm x 1 cm stamps and stored in a closed container for later use. The glass object carrier was also cut into 1 cm x 1 cm pieces, which were stored separately. Before use, these glass substrates were cleaned with ethanol in an ultrasonic bath for 5 min and dried in a nitrogen flow. In order to improve their wettability, PDMS stamps and glass substrates were treated with air plasma for 1 min at 0.2 mbar and a power of 100 or 300 W, respectively. Immediately before the printing procedure, the stamp was spin coated with 60 µL of polymer ink at 4000 rpm for 1 min, where the concentration of ink was varied between 1 and 3 wt%. A monolayer of MF particles was prepared by drop casting 5 µL of a 1 wt% aqueous particle dispersion on to the object carrier and subsequent drying under nitrogen flow at room temperature (RT) for 10 min.

Sandwich Microcontact Printing: In this procedure, the first PDMS stamp, coated with PMVEMA, was pressed against a monolayer of MF particles on the object carrier. To generate another patch made of PEI, the second inked stamp was pressed against the layer of monopatchy particles immobilized on the first stamp due to adhesion to the PMVEMA ink layer. Finally, the bipatchy particles were released from the second stamp in acetone in an ultrasonic bath for 15 min at RT. The dispersion of patchy particles was centrifuged for 3 min at 11 000 rpm, the supernatant removed, and the particles washed three times in ethanol with subsequent separation from supernatant at 8000 rpm for 3 min. After the washing procedure, particles were collected in an Eppendorf tube for further characterization.

Fluorescence Microscopy: For monitoring the patchy particles, their self-assembly behavior, and further statistics, fluorescence microscopy has been used. To allow for clear visualization of PEI and PMVEMA patches, polymeric inks were prelabeled before µCP with FITC and Rhodamine 6G, respectively. A stock solution of fluorescent dye in ethanol with a concentration of 5 µg mL^{-1} was initially prepared and 20 µL of this solution added to 80 µL of the polymeric ink solutions and allowed to sit for 15 min. For imaging, a Leica DMi8 microscope at magnifications of 20, 40, and 63 has been used and the resulted images were processed via Leica Application Suite X software provided by Leica.

Scanning Force Microscopy: Characterization of the qualitative and quantitative properties of patches, such as thickness and diameter, symmetry and shape, was provided by SFM. The corresponding samples were prepared by drop casting patchy particles on a silicon wafer. Otherwise, the patchy particles were fixed on a PDMS stamp and studied by SFM. The imaging was done using a Bruker Dimension Icon with Tapping Mode in air and ($k = 42$ Nm^{-1}, $f_0 = 300$ kHz) and the images were analyzed by Nanoscope Analysis software.

Scanning Electron Microscopy: Further information about the surface properties of patches such as morphology, roughness, and also the patch diameter was provided by SEM. A Gemini SEM 300 (Fa Zeiss) with a SE2-Detector at an acceleration voltage of 5 kV was used for imaging. The patchy particles were drop casted on a silicon wafer and sputtered using platinum with a thickness of 4 nm.

Supporting Information

Supporting Information is available from the Wiley Online Library or from the author.

Conflict of Interest

The authors declare no conflict of interest.

[1] Z. Zhang, S. C. Glotzer, *Nano Lett.* **2004**, *4*, 1407.
[2] É. Duguet, C. Hubert, C. Chomette, A. Perro, S. Ravaine, *C. R. Chim.* **2016**, *19*, 173.
[3] N. Patra, A. V. Tkachenko, *Phys. Rev. E* **2018**, *98*, 032611.
[4] E. W. Edwards, D. Wang, H. Möhwald, *Macromol. Chem. Phys.* **2007**, *208*, 439.
[5] E. Bianchi, C. N. Likos, G. Kahl, *ACS Nano* **2013**, *7*, 4657.
[6] S. C. Glotzer, M. J. Solomon, N. A. Kotov, *AIChE J.* **2004**, *50*, 2978.
[7] R. Guo, J. Mao, X.-M. Xie, L.-T. Yan, *Sci. Rep.* **2015**, *4*, 7021.
[8] S. Jiang, S. Granick, *Langmuir* **2009**, *25*, 8915.
[9] F. Sciortino, E. Bianchi, J. F. Douglas, P. Tartaglia, *J. Chem. Phys.* **2007**, *126*, 194903.
[10] Z. Gong, T. Hueckel, G.-R. Yi, S. Sacanna, *Nature* **2017**, *550*, 234.
[11] L. Sanchez, P. Patton, S. M. Anthony, Y. Yi, Y. Yu, *Soft Matter* **2015**, *11*, 5346.
[12] Y. Yi, L. Sanchez, Y. Gao, Y. Yu, *Analyst* **2016**, *141*, 3526.
[13] R. Mérindol, E. Duguet, S. Ravaine, *Chemistry - Asian J.* **2019**, *14*, 3232.
[14] P. Seidel, B. J. Ravoo, *Macromol. Chem. Phys.* **2016**, *217*, 1467.
[15] T. Kaufmann, M. T. Gokmen, C. Wendeln, M. Schneiders, S. Rinnen, H. F. Arlinghaus, S. A. F. Bon, F. E. Du Prez, B. J. Ravoo, *Adv. Mater.* **2011**, *23*, 79.
[16] T. Kaufmann, M. T. Gokmen, S. Rinnen, H. F. Arlinghaus, F. Du Prez, B. J. Ravoo, *J. Mater. Chem.* **2012**, *22*, 6190.
[17] T. Tigges, D. Hoenders, A. Walther, *Small* **2015**, *11*, 4540.
[18] T. Kaufmann, C. Wendeln, M. T. Gokmen, S. Rinnen, M. Becker, H. F. Arlinghaus, F. Du Prez, B. J. Ravoo, *Chem. Commun.* **2013**, *49*, 63.
[19] M. Zimmermann, D. John, D. Grigoriev, N. Puretskiy, A. Böker, *Soft Matter* **2018**, *14*, 2301.
[20] M. Zimmermann, D. Grigoriev, N. Puretskiy, A. Böker, *RSC Adv.* **2018**, *8*, 39241.

[21] D. John, M. Zimmermann, A. Böker, *Soft Matter* **2018**, *14*, 3057.

[22] F. Naderi Mehr, D. Grigoriev, N. Puretskiy, A. Böker, *Soft Matter* **2019**, *15*, 2430.

[23] T. Yamane, *Statistics: An Introductory Analysis*, Harper And Row, New York **1967**.

[24] M. Kosmulski, *J. Colloid Interface Sci.* **1998**, *208*, 543.

[25] E. Bichoutskaia, A. L. Boatwright, A. Khachatourian, A. J. Stace, *J. Chem. Phys.* **2010**, *133*, 024105.

[26] E. B. Lindgren, A. J. Stace, E. Polack, Y. Maday, B. Stamm, E. Besley, *J. Comput. Phys.* **2018**, *371*, 712.

[27] E. B. Lindgren, I. N. Derbenev, A. Khachatourian, H.-K. Chan, A. J. Stace, E. Besley, *J. Chem. Theory Comput.* **2018**, *14*, 905.

[28] A. J. Stace, A. L. Boatwright, A. Khachatourian, E. Bichoutskaia, *J. Colloid Interface Sci.* **2011**, *354*, 417.

[29] E. B. Lindgren, B. Stamm, Y. Maday, E. Besley, A. J. Stace, *Philos. Trans. R. Soc., A* **2018**, *376*, 20170143.

2000442 (9 of 9)